Research paper

Comparative study between PI, FLC, SMC and Fuzzy sliding mode controllers of DFIG wind turbine

Zahira Bouguerra [*]

Faculty of sciences and technology, University of Mohamed El Bachir El Ibrahimi, Bordj Bou Arréridj

ARTICLE INFO	ABSTRACT
	In speed control, double-fed-induction generator (DFIG) has attracted attention in wind energy conversion systems (WECs). These systems can offer higher performances by controlling converters that connect the generator windings to the grid network. Therefore, different control strategies have been used. We can find the proportional integral (PI) and sliding mode control (SMC) which offer better performances. However, PI has constant gains that can't change with the external variation and SMC has a chattering problem. Therefore, a hybrid control system that combines fuzzy logic control (FLC) and SMC to perform fuzzy sliding mode control (FSMC) is proposed. The hybrid system can improve the FLC and SMC robustness. The DFIG modeling and each of the control strategies have been detailed. To demonstrate the effectiveness of the control strategies, a comparative study of different control strategies (PI, FLC, SMC and FSMC) is described and performed using MATLAB/Simulink software. The results obtained from the present study show that FSMC is more robust and efficient than the other controllers (PI, FLC and SMC). It has high performances (low settling time, high steady state accuracy) assuring a perfect power decoupling with minimal ripples and errors.

1. INTRODUCTION

The environmental impacts and diminishing reserve of fossil fuel is forcing the power system planners across the globe to look for increased use of renewable energy (Evangelista et al., 2013). Among them, wind energy has drawn the large attention in the word. This is due, particularly, to the evolution of power semiconductors, decreasing equipment costs, and the development of the wind turbines industry which tends to have capacity of 2 MW or more (Achouri et al., 2011). In wind generation systems,

[*] *Corresponding author, E-mail address: zahira.bouguerra@univ-bba.dz*

variable-speed variable-frequency based electrical generators can increase the energy production, with the flexibility of operating under wide wind conditions, simultaneously reducing the stress on the mechanical subsystem and offering maximum efficiency at al wind velocities (Shanti et al., 2017). In the modern wind energy conversion systems (WECs), doubly fed induction generator (DFIG) has a crucial role in variable speed technology (Zamzoum et al., 2018). The use of doubly fed induction generator (DFIG) has increased tremendously due to its easy maintenance with good reliability, low cost, and simple construction (Benbouhenni et al. 2020).

In the WEC system, power output is affected by geographical and metrological conditions. Thus, the power electronic plays a significant role in forcing the system to produce maximum power despite internal or external variations. In addition, they are used to match the characteristics of wind turbines with the requirements of grid connections, including frequency, voltage, control of active and reactive power, harmonics, etc. (Chen et al. 2009). The DFIG rotor is interconnected to the grid through tow converters and directly from the stator winding. Where, the rating of the power electronic converter is only 25–30% of the generator capacity (Li and Chen, 2008). Many different structure and control algorithms are developed to control DFIG-based wind turbine system's behavior during normal operation, the most control used is based on vector control (Field oriented control) as proposed in (Krim et al., 2018). PI control has fixed gains which can't adjust with the extern variations. In fact, wind energy system has high nonlinearity obtained from uncertainties, wind speed turbulence, and the changes in wind system parameters (Krim et al. 2018). For this reason, nonlinear controls have been developed to be not very sensitive to wind speed and parameters variation, such as sliding mode controller (Serhoud and Benattous, 2011, 2012; Azzouz et al. 2019; Bouguerra and Benfdila, 2023), fuzzy logic controller (Belaimeche et al., 2018; Cheikh et al., 2013; Djoudi et al., 2021), Artificial Neural Networks (Benbouhenni, 2020), fuzzy sliding mode control (Benmeziane et al., 2019), H_∞ Controller (Saihi et al., 2020), etc.

In this work, a comparative study between four control strategies is developed using proportional-integral (PI), SMC, FLC and FSMC controllers to independently control DFIG powers. The PI controller is very simple to implement but is not sensitive to external or internal variations that can significantly degrade system performance. The SMC algorithm includes the DFIG parameters, so when these parameters change, the SMC lows remain the same, resulting in a significant error. In addition, the added discontinuous signal produces strong ripples causing chattering. To overcome this problem, hybridization between SMC and FLC is proposed. Replacing the sign(S) in the SMC controller by the FLC control can significantly improve the performance of this control and eliminate the chattering phenomena. To improve the effectiveness of FSMC controller, a comparative study is established under variations of wind speed and DFIG parameters. The performances of PI, FLC, SMC and FSMC controls are compared using reference tracking and robustness criteria using the MTLAB/Simulink software.

2. SYSTEM DESCRIPTION

The WECs schema is described in figure 1. A wind turbine drives the rotor of DFIG by mean multiplier gearbox (GB), and its stator is immediately interconnected to the grid. A comparative analysis is made between four control strategies (PI, SMC, FLC, and FSMC) commanding DFIG powers, to compare the performances of the system according the reference tracking, robustness and rejection disturbance.
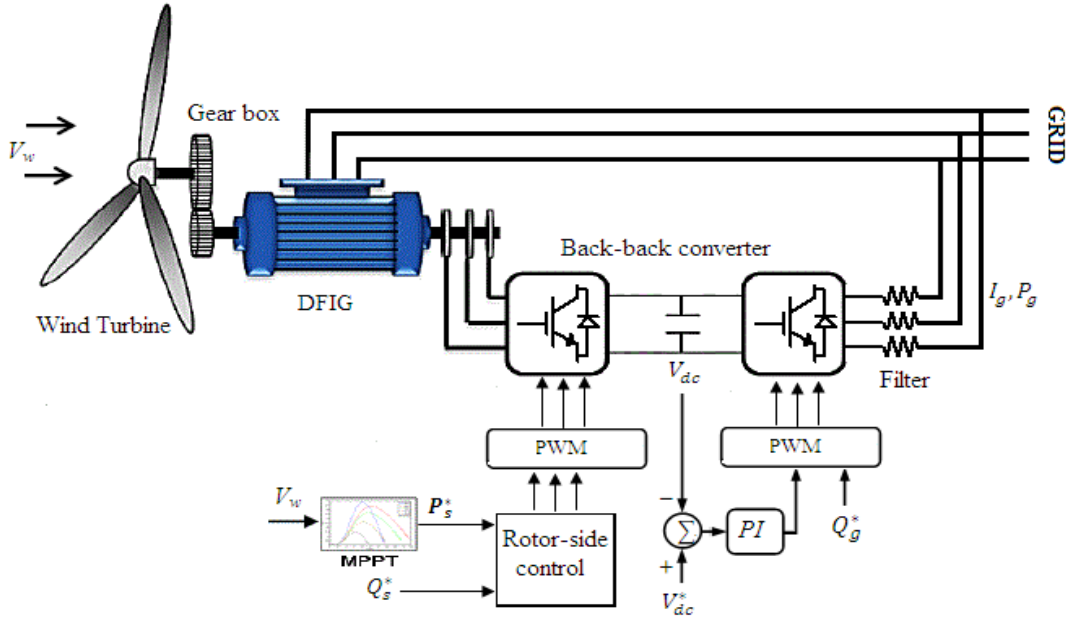
Fig 1. WECs conversion system based on DFIG

3. SYSTEM MODELLING

3.1 Aerodynamics modeling

The wind speed turns the blades which produces a mechanical power in the shaft. Then, the DFIG transforms it in electrical power. The turbine power is given by equation (1) (Aissou et al., 2015):

$$P_t = \frac{1}{2}\rho \cdot C_p(\lambda, \beta).S \cdot V_w^3 \qquad (1)$$

The power coefficient C_p is calculated by the following equations (Tir and Abessemed, 2014):

$$C_p(\lambda, \beta) = 0.5176 \left(\frac{116}{\lambda_i} - 0.4\beta - 5\right) e^{\frac{-21}{\lambda_i}} + 0.0068 \qquad (2)$$

$$\frac{1}{\lambda_i} = \frac{1}{\lambda + 0.08\beta} - \frac{0.035}{\beta^3 + 1} \qquad (3)$$

The tip speed ration or relative λ is the ratio between the linear blade speed and the speed of the wind (Tir and Abdessemed, 2014):

$$\lambda = \frac{R \cdot \omega_t}{V_w} \qquad (4)$$

By keeping λ at its optimal value (λ_{opt}) the coefficient is at its maximum then as shown in figure (2), the optimal power can calculate by the following equation:

$$P_s^* = \frac{1}{2}\rho \cdot C_{pmax}(\lambda_{opt}).S \cdot V_w^3 \qquad (5)$$

As shown in figure (2), for each wind speed the system has an optimum rotational speed which gives the maximum power. The main objective of RsC control is to find this point of maximum power which means to find the optimum rotation speed.
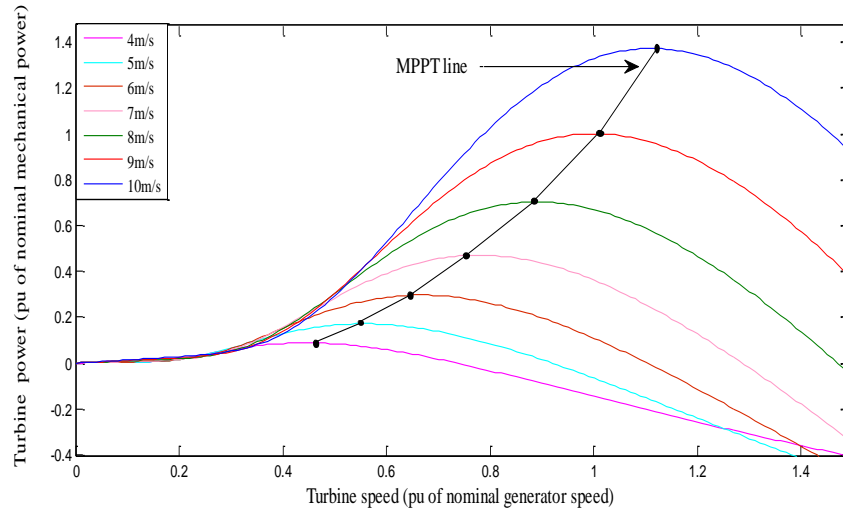
Fig 2. The mechanical power for different wind speed values

3.2 DFIG modeling

The DFIG consists of two essential parts; the first one is the stationary part (the stator) which it is directly connected to the grid. The second one is the rotor that is connected mechanically to the turbine through a gearbox and it is connected too to the back-to-back converters via a rings system. The both parts are consisted by three windings with a diphase angle of 120°. Using Park transformation, the rotor, stator voltages of the DFIG are given by the following equation:

$$\begin{cases} V_{sd} = R_s I_{sd} + \frac{d\varphi_{sd}}{dt} - \omega_s \varphi_{sq} \\ V_{sq} = R_s I_{sq} + \frac{d\varphi_{sq}}{dt} + \omega_s \varphi_{sd} \\ V_{rd} = R_r I_{rd} + \frac{d\varphi_{rd}}{dt} - \omega_r \varphi_{rq} \\ V_{rq} = R_r I_{rq} + \frac{d\varphi_{rq}}{dt} + \omega_r \varphi_{rd} \end{cases} \tag{6}$$

With: $\omega_r = \omega_s - p\omega_t$

When, the flux is given in equation (7):

$$\begin{cases} \varphi_{sd} = L_s I_{sd} + L_m I_{rd} \\ \varphi_{sq} = L_s I_{sq} + L_m I_{rq} \\ \varphi_{rd} = L_r I_{rd} + L_m I_{sd} \\ \varphi_{rq} = L_r I_{rq} + L_m I_{sq} \end{cases} \tag{7}$$

The stator powers are given in equation (8):

$$\begin{cases} P_s = I_{sd} V_{sd} + V_{sq} I_{sq} \\ Q_s = V_{sq} I_{sd} - V_{sd} I_{sq} \end{cases} \tag{8}$$

The electromagnetic torque (C_{em}) equation is:

$$C_{em} = -p \frac{L_m}{L_s} (\varphi_{sq} I_{rd} - \varphi_{sd} I_{rq}) \tag{9}$$

4. INDIRECT FIELD-ORIENTED CONTROL

After the DFIG modeling, the mechanical model is non-linear and it is strongly coupled which makes its control very difficult and complex. So, to simplify this problem with a great efficiency, the application of vector control is necessary. When, the principle of the vector control is to assimilate the behavior of an induction machine to a DC machine, to control the flux and the torque independently. In result, the currents I_{rq}, I_{rd} are responsible for command the active and reactive powers respectively. Under stator field orientation, the stator field vector is aligned with the d-axis as shown in figure (3):
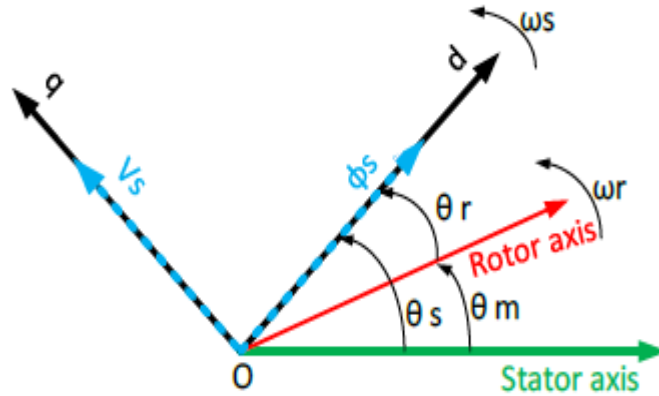
Fig 3. Stator field orientation of DFIG

The stator's flux and voltages are given in the following equations:

$$\begin{cases} \varphi_{sd} = \varphi_s \\ \varphi_{sq} = 0 \end{cases} \tag{10}$$

$$\begin{cases} V_{sd} = 0 \\ V_{sq} = V_s = \omega_s \varphi_s \end{cases} \tag{11}$$

By substituting the equation (10) in equation (7), the stator currents can be calculated as shown:

$$\begin{cases} I_{sq} = -\frac{L_m}{L_s} I_{rq} \\ I_{rd} = -\frac{L_m}{L_s} I_{rd} + \frac{V_s}{\omega_s L_m} \end{cases} \tag{12}$$

The replacing of equation (12) in equation (8) gives the flowing equation:

$$\begin{cases} P_s = -\frac{3L_m}{2L_s} V_s I_{rq} \\ Q_s = \frac{3V_s^2}{2L_s \omega_s} - \frac{3L_m}{2L_s} V_s I_{rd} \end{cases} \tag{13}$$

The DFIG voltages are expressed as:

$$\begin{cases} V_{rd} = R_r I_{rd} + L_r \sigma \frac{dI_{rd}}{dt} - g\omega_s L_r \sigma I_{rq} \\ V_{rq} = R_r I_{rq} + L_r \sigma \frac{dI_{rq}}{dt} + g\omega_s L_r \sigma I_{rd} + g\frac{L_m V_s}{L_s} \end{cases} \tag{14}$$

The electromagnetic torque is given by this equation:

$$C_{em} = -p\frac{3L_m V_s}{2L_s \omega_s} I_{rq} \tag{15}$$

When $\sigma = 1 - \frac{L_m^2}{L_s.L_r}$

After the powers equation (13), the rotor currents can be expressed in equation (16):

$$\begin{cases} I_{rq}^* = -\frac{2L_s}{3L_m}P_s \\ I_{rd}^* = -\frac{2L_s}{3L_mV_s}Q_s + \frac{V_s}{\omega_s L_m} \end{cases} \tag{16}$$

The indirect field-oriented control (IFOC) using PI regulator is shown in figure 4.
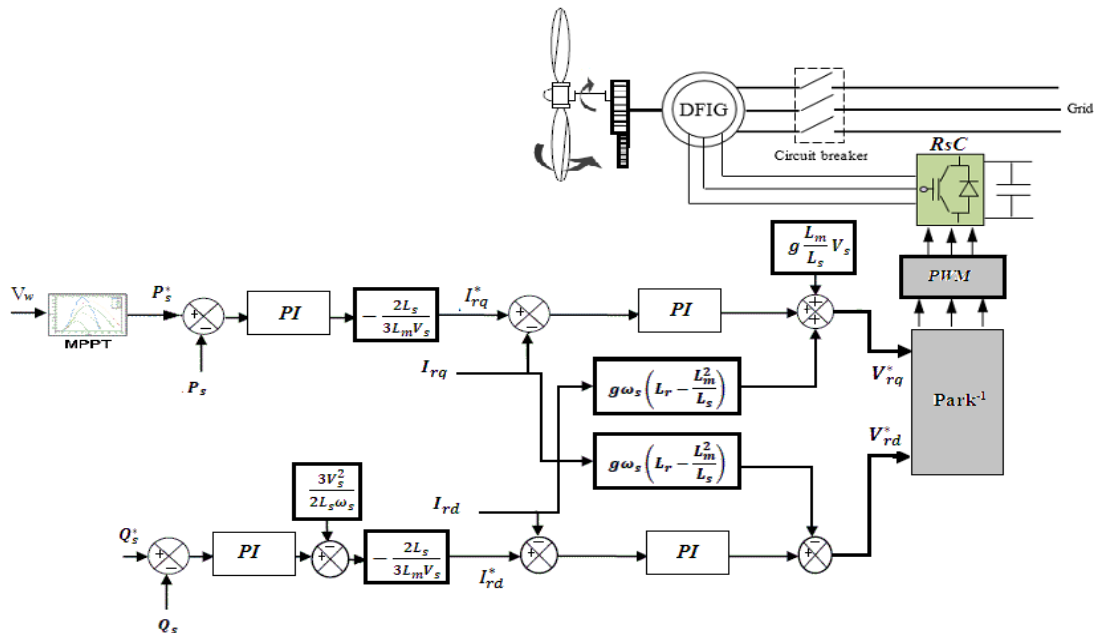
Fig 4. DFIG schema using IFOC (PI) controller

5. FUZZY LOGIC CONTROL

Due to its high efficiency and performance under external changes, the FLC technique became one of the most widely used controller in renewable energy systems Bouguerra and Benfdila, 2021). According to available information's, Fuzzy logic control (FLC) is able to control nonlinear, uncertain systems using a fuzzy model, rule and logic language variation to give very satisfactory performances. Fuzzy controller schema is illustrated in Figure 6, which has two inputs (e, de) and one output (u).
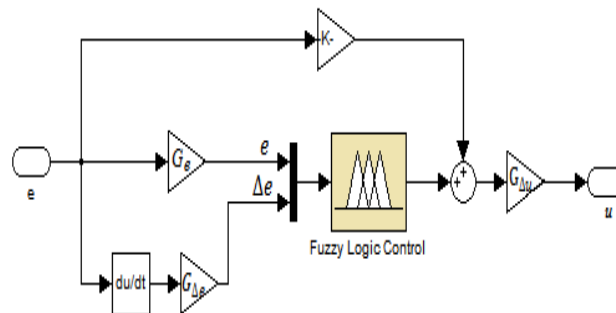
Fig 5. FLC structure

Figure 7 represents the membership functions and the Table 2 shows the rule of FLC controller. The symbols BP, MP, P, ZE, N, MN, BN signify respectively Big Positive, middle Positive, Positive, Zero, Negative , Middle Negative, Big Negative.
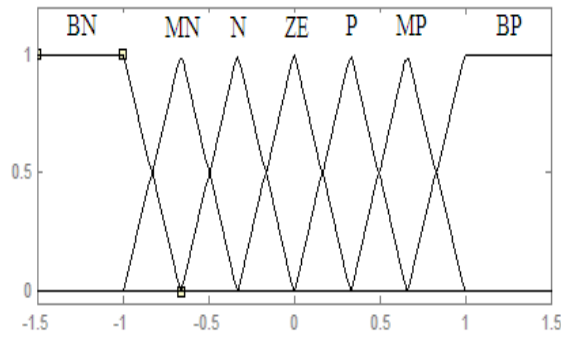
Fig 6. $e, \Delta e, \Delta u$. Membership functions

Table 1. Rule bases of FLC controller

u		de						
		BN	MN	N	ZE	P	MP	BP
	BN	BN	BN	BN	BN	MN	N	ZE
	MN	BN	BN	BN	MN	N	ZE	P
	N	BN	BN	MN	N	ZE	P	MP
e	ZE	BN	M N	N	ZE	P	MP	BP
	P	MN	N	ZE	P	MP	BP	BP
	MP	N	ZE	P	MP	BP	BP	BP
	BP	ZE	P	MP	BP	BP	BP	BP

6. SLIDING MODE CONTROL

Due to its simple implementation, strong robustness and high ability to handle disturbances, the sliding mode control is considered as a robust controller of nonlinear systems. The principle of this technique is made by applying a discontinuous signal (sign(S(X))) to oblige the system to slide around the chosen sliding surface.
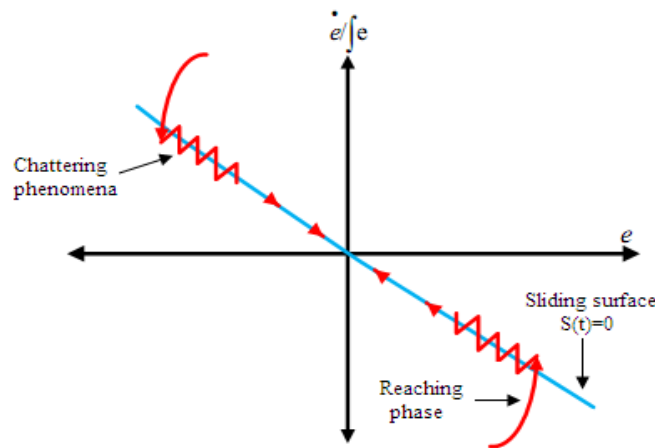
Fig 7. The interpretation of sliding mode control

The SMC control is calculated by adding the discontinuous component to the equivalent control which is calculated from the chosen sliding surface. This SMC control is given in equation (17):

$$u = u_{eq} + u_n \tag{17}$$

The sliding surfaces are given in equation (18):

$$\begin{cases} S(P) = I_{rq}^* - I_{rq} \\ S(Q) = I_{rd}^* - I_{rd} \end{cases} \tag{18}$$

In sliding mode control, the derivatives of surfaces must be equal to zero:

$$\begin{cases} \dot{S}(P) = \dot{I}_{rq}^* - \dot{I}_{rq} = 0 \\ \dot{S}(Q) = \dot{I}_{rd}^* - \dot{I}_{rd} = 0 \end{cases} \tag{19}$$

After the equation (14), the currents expression is retired as shown in this function:

$$\begin{cases} \dot{I}_{rd} = \frac{1}{L_r \sigma}\left(V_{rd} - R_r I_{rd} + g\omega_s L_r \sigma I_{rq}\right) \\ \dot{I}_{rq} = \frac{1}{L_r \sigma}\left(V_{rq} - R_r I_{rq} - g\omega_s L_r \sigma I_{rd} - g\frac{L_m V_s}{L_s}\right) \end{cases} \tag{20}$$

By replacing the equation (16) and (20) in equation (19), that gives the equivalent commands of sliding mode control as detailed in equation (21):

$$\begin{cases} V_{rq}^{eq} = -\frac{2L_s L_r \sigma}{3L_m V_s}\dot{P}_s^* + R_r I_{rq} + g\omega_s L_r \sigma I_{rd} + g\frac{L_m.V_s}{L_r} \\ V_{rd}^{eq} = -\frac{2L_s L_r \sigma}{3V_s L_m}\dot{Q}_s^* + R_r I_{rd} - g\omega_s L_r \sigma I_{rq} \end{cases} \tag{21}$$

We consider that:

$$V_{rd,rq}^* = V_{rd,rq}^{eq} + Ksign(S_{PQ}) \tag{22}$$

The DFIG model using SMC controller is illustrated in figure 8.
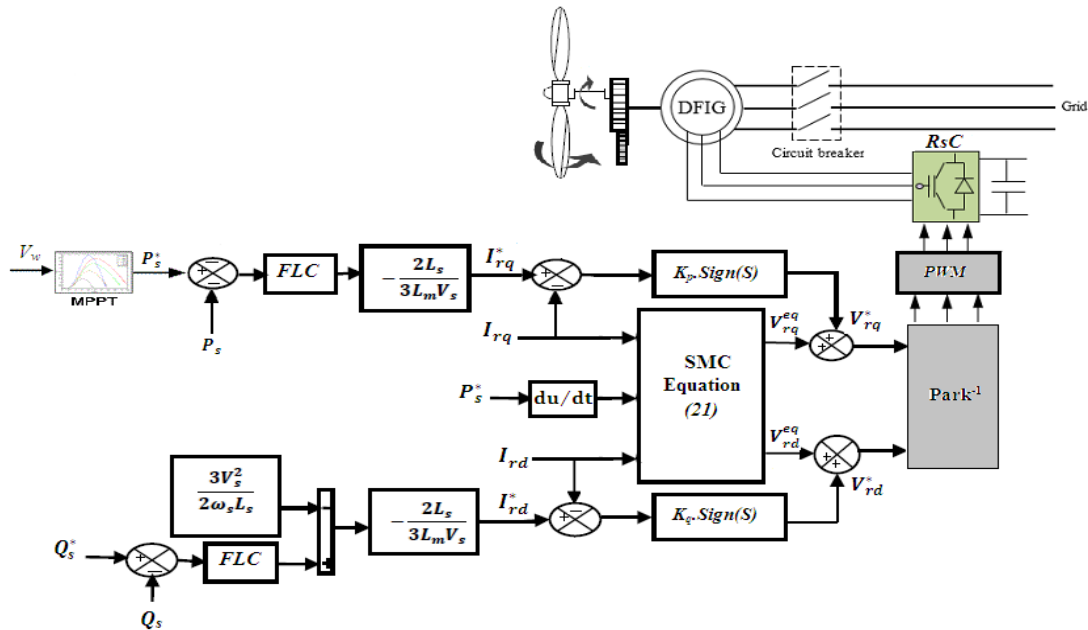
Fig 8. DFIG schema using SMC controller

7. FUZZY SLIDING MODE CONTROL

The addition of the discontinuous control signal to sliding surface provokes chattering phenomenon which can affect many damages to the mechanical components. Therefore, a FSMC control is established which associates the SMC with the FLC to improve the SMC performances. FSMC replaces $Ksign(S(X))$, by fuzzy term as expressed in (22).

$$u = u_{eq} + u_{fuzzy} \tag{22}$$

The detailed DFIG schema using FSMC controller is shown in figure 9.

Fig 9. Fuzzy sliding mode control

8. SIMULATION RESULTS

A comparative study is presented below using (PI, FLC, SMC and FSMC) to control independently the DFIG powers based on WECs under wind speed and parameters variations in terms of power reference tracking, THD of the Stator Current, the dynamic response, static error, precision overshoot and robustness. The system parameters are listed in Table 2.

Table 2. WECs parameters

Wind turbine		DFIG	
Gearbox ratio (G)	90	Power	1.5 MW
Blade radius (R) m	35.25 m	Number of pole pairs (p)	2
Moment of Inertia (J)	1000 kg m2	Rotor resistance (R_r)	0.021 Ω
		Stator inductance (L_s)	0.0137 H
		Rotor inductance(L_r)	0.0136 H
		Mutual inductance (L_m)	0.0135 H

8.1 Reference tracking

The first series of tests are performed using a realistic wind speed to verify the robustness of system during this disturbance. The reference value of the active power (P_{sref}) is calculated by the MPPT strategy and the reactive power value is kept at zero ($P_{sref} = 0$) to ensure unity power factor. After the decoupling process applied, the active power and the electromagnetic torque are depending directly with the quadrature component of the DFIG rotor current (I_{rq}) as detailed in equations (13) and (15). consequently, P_s and C_{em} vary in the same manner as I_{qr}. When, the reactive power is proportional to the direct component of DFIG rotor current (I_{dr}) as proved in equation (13). That explains the same shape of Q_s with I_{dr}. This means that the decoupling has been successfully achieved.

In figure 10, the powers follow their references values in infinite time with a good accuracy and respected decoupling (the active power is negative, which means that the DFIG operates as a generator). The amplitudes of ripples of FSMC and FLC are smaller and occur in a shorter period compared to ripples obtained for the PI and SMC and PI controllers.

The stator and rotor currents are sinusoidal with a frequency of 50Hz and their magnitudes vary with the variation of wind speed as shown in figures (14 and 15). The total harmonic distortion (THD) of stator currents of the utilized controllers is less than 1% (figure 16); the best THD is obtained by FLC and FSMC controllers (0.28% and 0.33% respectively), which means that a good quality of energy is injected to the grid.
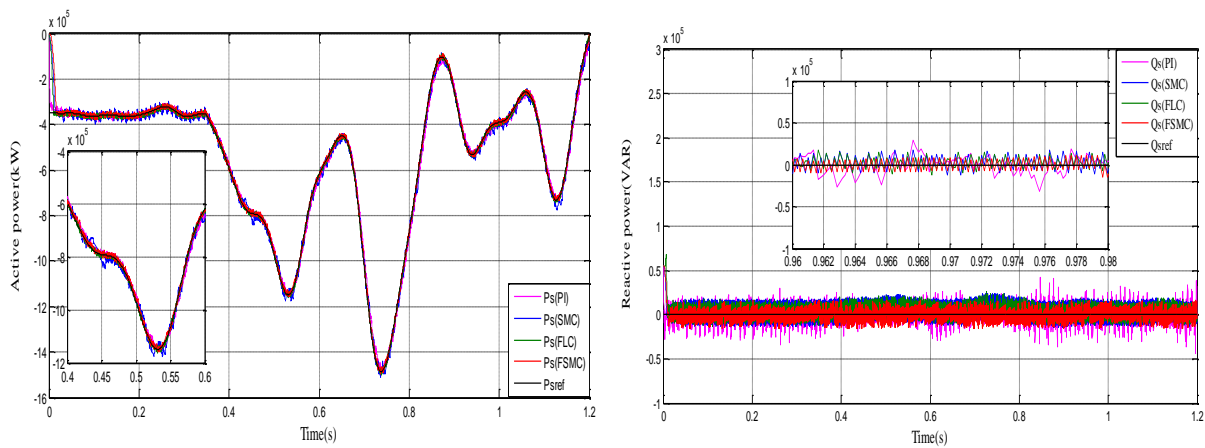
Fig 10. Active and reactive behavior
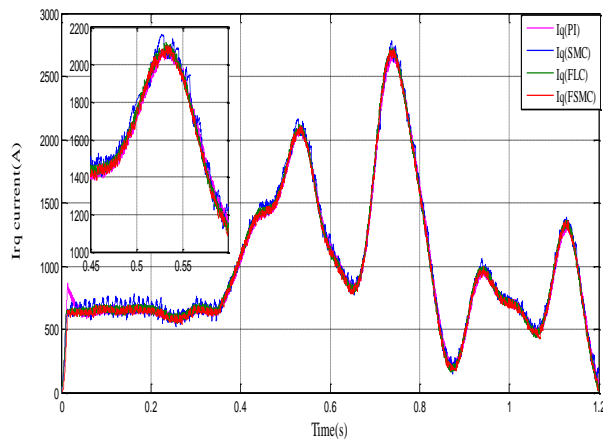
Figure 11. Quadrature current of the rotor   Figure 12. Direct current of the rotor
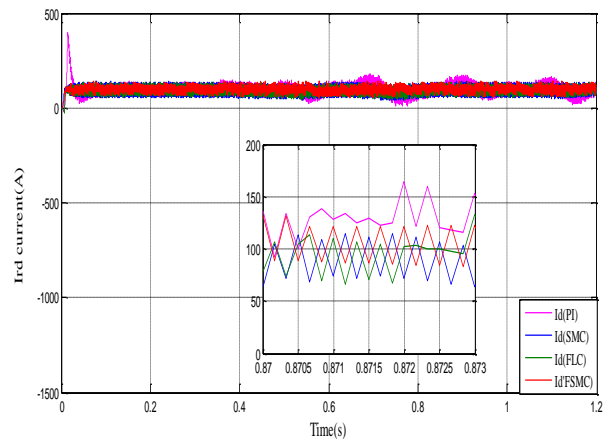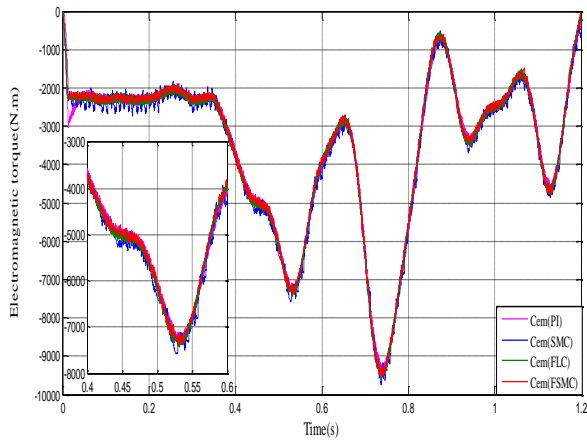
Fig 13. Electromagnetic torque
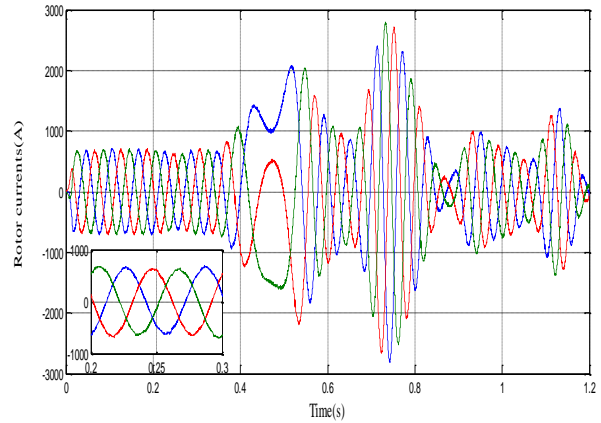
Fig 14. DFIG rotor currents
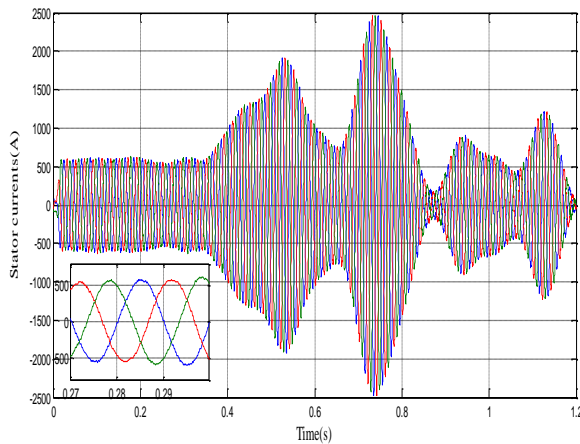
Fig 15. DFIG Stator Current
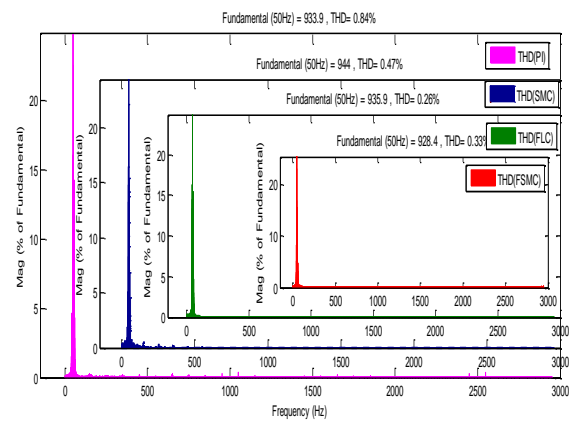
Fig 16. THD of stator currents

8.2 Robustness

The second series of tests is executed using a stepped wind to visualize the transient and steady state responses of different control applied to the WECs-DFIG. We are interested in comparing the robustness of the different controllers (PI, FLC, SMC, FSMC) against parameters variation such as the inductances L_s, L_r the mutual inductance L_m and resistances R_s, R_r. The impact of rotor inductance $L_S(30\%)$ is displayed in figure (17). Figure 18, 19 and figure 20 display simulation results when several parameters change at the same time. Figure 12 ($R_r + 50\%$, $L_r + 30\%$, $L_m + 10\%$), figure 19 (50% of R_r, R_s, +10 L_m and 30%L_r), figure 20 ($R_r + 100\%$, $R_s + 100\%$, $L_r + 10\%$ and $L_m - 5\%$)

First, the MATLAB / simulink results show that the active/reactive power decoupling is maintained and respected. In addition, the coupling effect has been watched at $t = 0.5s$ and at $t = 1.7s$ in active power with PI regulator. These oscillations appear if a considerable change is applied to reactive power (increase from $-5VAR$ to $0VAR$ at $t = 0.5s$ and decrease from 5VAR to 0VAR at $t = 1.7s$), also, this coupling effect appears clearly in reactive power only with PI and FLC controllers (at $t = 1s, 2s, 3s$).

Secondly, we note a faster response for the FSMC (t_s(settling time) $= 0.009s$), FLC ($t_s = 0.0093s$) and SMC ($t_s = 0.0125s$), the responses with these regulators are correctly followed without any overshoots. The responses with the PI controller have evolved to a steady state with significant response time (0.09s), error and overshoots compared to other controllers. Between t=3 and 4s, the total power produced by the DFIG is the maximum that the DFIG can produce (1.5MW), the system using the PI controller suffers from producing it completely with the variation of parameters as presented in figures

(17, 20), with of high ripples and significant error in reactive power. In figure 20, a negligible error and enlarged ripples are shown with the SMC controller to satisfy the 1.5 MW demand. In reactive power, an error is displayed with all three controllers (PI, FLC and SMC) due to a high active power demand (1.5 MW) without any error in FSMC control, demonstrating the high robustness of the FSMC compared to other controllers.
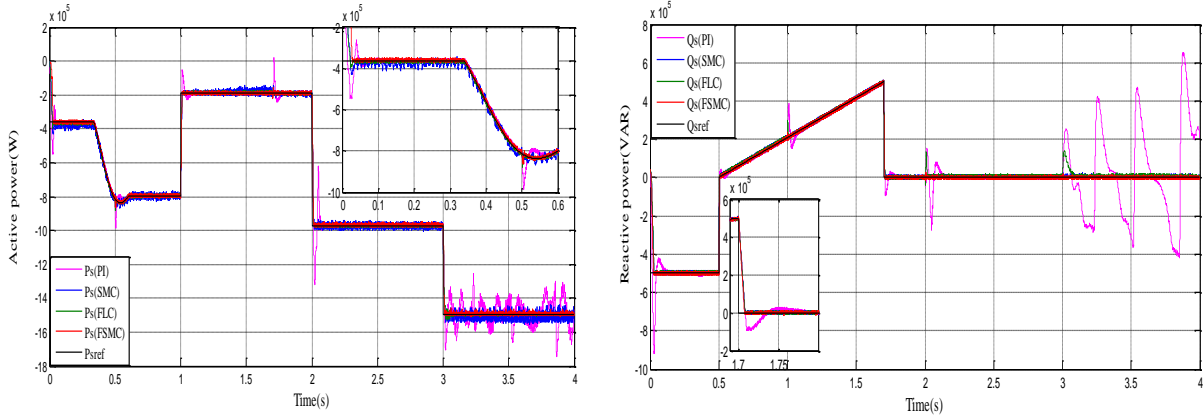
Fig 17. Powers behavior with: 30% of L_s variation
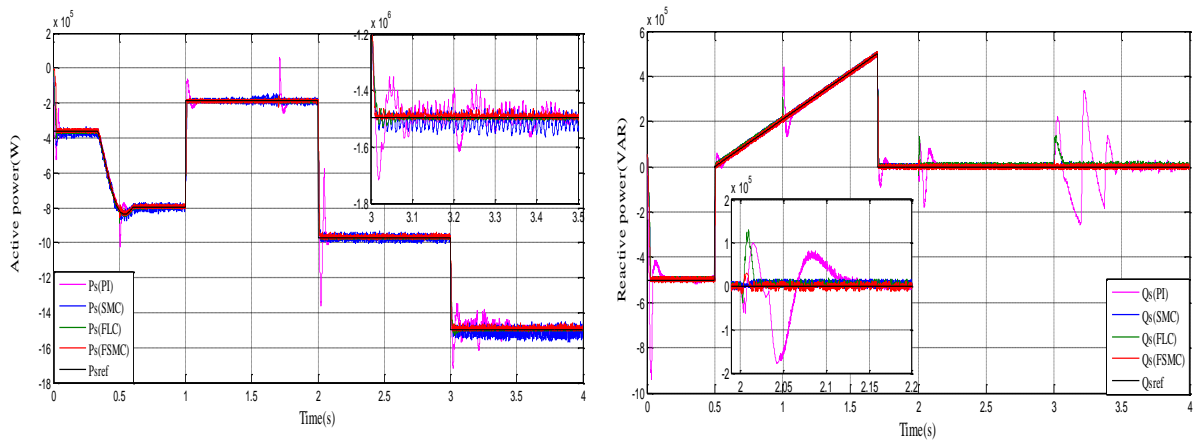
Fig 18. Powers behavior with: 50% variation of R_r, R_s and 30% variation of L_r
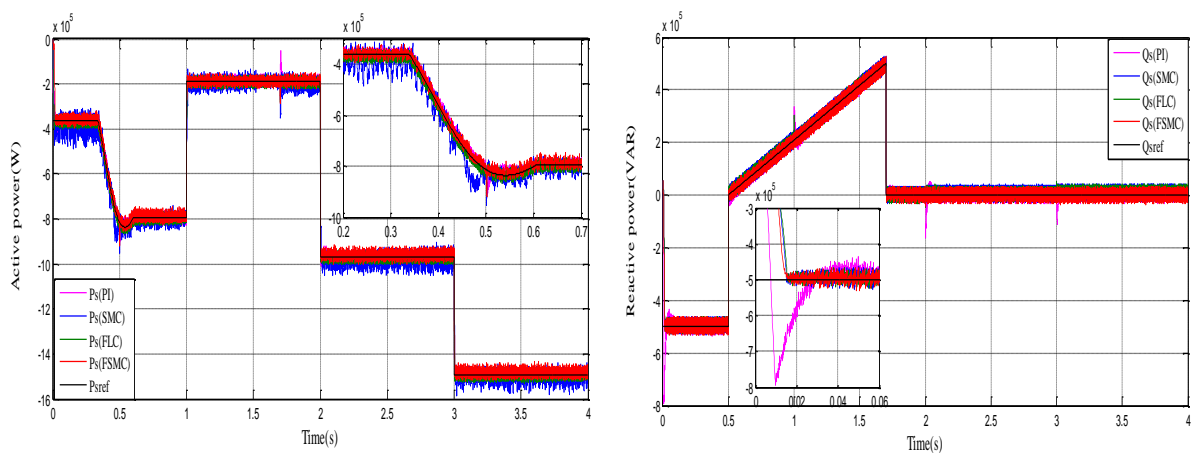
Fig 19. Powers behavior with: 50% of R_r, R_s, +10 L_m and 30% L_r
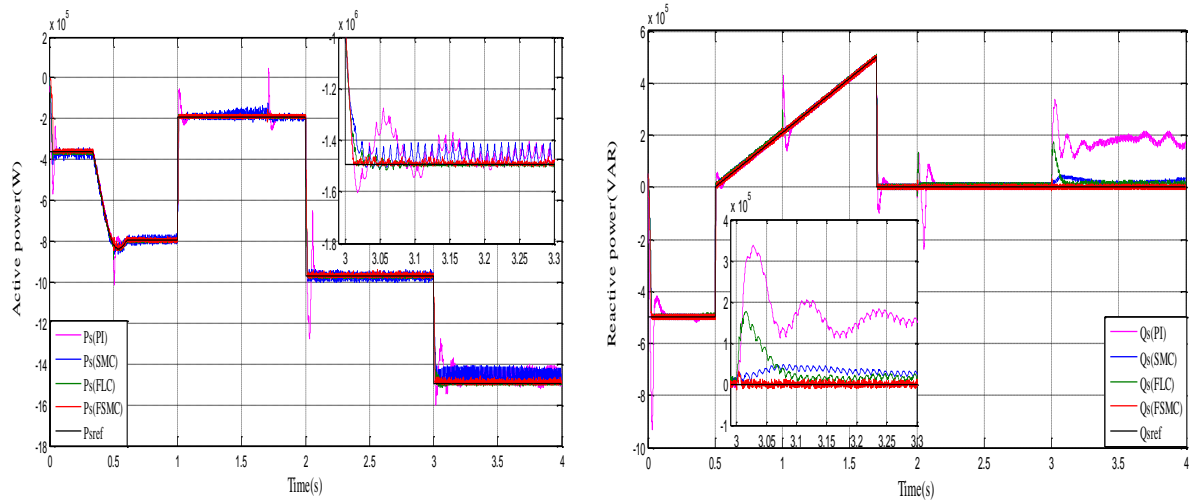
Fig 20. Powers behavior with: 100% variation of R_r, R_s, +10% variation of L_r, L_s and -5% variation of L_m

Table 3 compares the performances of these four controllers, PI controller takes a long time to follow its reference with undesirable maximum overshoots, a considerable error and a medium robustness against the parameters variation. This is due to the fixed gains which can't change with the variations of internal and external parameters. SMC presents a high robustness compared to PI regulator with a quick response time and without any overshoot. But it shows high oscillations due to the use of discontinuous control single. FLC has presented a high performance compared to PI and SMC. However, FSMC can resist this parametric variation without any overshoot or error, giving the higher robustness and performances against any parameters variations.

Table. 3 Comparative of the performances of applied controllers

Performances	Response time(s)	Overshoot (%)	Robustness	Precision	Set-point tracking
PI	0.09	31%	Medium	Medium	Good
SMC	0.0125	-	Strong	Good	Very Good
FLC	0.0093	-	strong	Good	Very Good
FSMC	0.009	-	Excellent	High	Very good

9. CONCLUSION

The control of DFIG wind turbine has been studied in this paper. A PI, SMC, FLC and FSMC controllers are applied to control independently the active and reactive power to improve the system performances. The obtained results show that the PI, FLC, SMC and FSMC controllers function well under normal conditions. However, in the case of parameters variation, the PI degrades the system performances because it has fixed gains which are incapable to track perfectly the power references when parameters change. SMC has a chattering problem. FLC shows less oscillation than PI and SMC controllers. As a result, the FSMC controller gives very high performances toward sensitivity to perturbation under parameters variation with minimal ripples and error compared to all other regulators.

NOMENCLATURE

Turbine			
P_t	Turbine power	β	pitch angle
ω_t	Turbine rotational speed	R	Radius of turbine rotor
ρ	Air density	λ	Tip speed ratio
C_p	Power coefficient	V_w	Wind speed
S	Area swept by turbine blades	λ_{opt}	Optimal value of tip speed ratio
DFIG			
V_{sd}, V_{sq}	d-q stator voltages	R_r	Rotor phase resistance
$\varphi_{sd}, \varphi_{sq}$	d-q stator flux	R_s	Stator phase resistance
$\varphi_{rd}, \varphi_{rq}$	d-q rotor flux	ω_s	Stator angular frequency
V_{rd}, V_{rq}	d-q rotor voltages	ω_r	Rotor angular frequency
I_{sd}, I_{sq}	d-q stator currents	L_s	Stator inductance
I_{rd}, I_{rq}	d-q rotor currents	L_r	Rotor inductance
P_s	Stator active power	C_{em}	electromagnetic torque
Q_s	Rotor active power	p	Number of pole pair

REFERENCES

Achouri F, Achour A.Y, Mendil B. (2011). A PMSG wind turbine control based on passivity. Revue des Energies Renouvelables, ICESD'11, Adrar, pp. 261–270.

Aissou S, Rekioua D, Mezzai N, Rekioua T, Bacha S. (2015). Modeling and control of hybrid photovoltaic wind power system with battery storage, Energy Conversion and Management, Vol. 89, pp. 615-625. doi: 10.1016/j.enconman.2014.10.034.

Ait Madi A, Addaim A, Intidam Abdeslam A, Laafou J. (2020). Dynamic Modeling and Improved Control of a Grid-Connected DFIG Used in Wind Energy Conversion Systems. Mathematical Problems in Engineering, Vol. 2020. doi: 10.1155/2020/1651648.

Azzouz S, Messalti S, Harrag A. (2019). Innovative MPPT controller for extraction of maximum power from variable wind turbine. przegląd elektrotechniczny, Vol. 95, N°8. doi:10.15199/48.2019.08.26.

Belaimeche F. Z, Bentaallah A, Massoum S, Wira P. (2018). A comparative study between a simplified fuzzy PI and classic PI input-output linearizing controller for the wind-turbine doubly fed induction generator. elektro tehniški vestnik, Vol. 85, N° 4, pp. 142–148.

Benbouhenni H, Boudjema Z, Belaidi A. (2020). DPC Based on ANFIS Super-Twisting Sliding Mode Algorithm of a Doubly-Fed Induction Generator for Wind Energy System. Journal Européen des Systèmes Automatisés, Vol. 53, N°1, pp. 69–80. doi: 10.18280/jesa.530109.

Benbouhenni H. (2020). Twelve Sectors DPC Control Based on Neural Hysteresis Comparators of the DFIG Integrated to Wind Power, Tecnica Italian journal of engineering science , Vol. 64, N°2, pp. 347–353. doi: 10.18280/ti-ijes.642-433.

Benmeziane M, Zebirate S, Chaker A, Boudjema Z. (2019). Fuzzy sliding mode control of doubly-fed induction generator driven by wind turbine, International, Journal of Power Electronics and Drive System (IJPEDS), Vol. 10, N°3, pp. 1592–1602. doi: 10.11591/ijpeds.v10.i3.pp1592-1602.

Bouguerra Z, Benfdila A. (2021). A Comparative study of individual and hybrid renewable energy systems (photovoltaic, Wind energy and its hybridization) controlled by fuzzy logic control. Journal of Engineering Science and Technology Review, Vol. 14, N°5, pp. 180 –186. doi:10.25103/jestr.145.21.

Bouguerra Z, Benfdila A. (2023). DFIG Wind turbine controlled by sliding mode control and fuzzy sliding mode control, Algerian journal of signals and systems, Vol. 8, pp. 8–14. doi:10.51485/ajss.v8i1.180.

Cheikh R, Menacer A, Drid S, Tiar M. (2013). Application of fuzzy logic control algorithm as stator power controller of a grid-connected doubly-fed induction generator. Frontier in Energy, Vol. 7, N°1, pp. 49–55. doi:10.1007/s11708-012-0217-7.

Chen Z, J. Guerrero M, Blaabjerg F. (2009). A Review of the state of the art of power electronics for Wind turbines. IEEE transactions on power electronics, Vol. 24, N°8. DOI: 10.1109/TPEL.2009.2017082.

Djoudi O, Belaid S. L, Tamalouzt S. (2021). A high degree of direct torque control applied to a grid-connected wind energy system based on a DFIG, Journal of Renewable Energies, ICREATA'21, Adrar, pp. 81–91. doi: https://doi.org/10.54966/jreen.v1i1.1042.

Evangelista C, Valenciaga F, Puleston P. (2013). Active and reactive power control for wind turbine based on a MIMO 2-sliding mode algorithm with variable gains. IEEE transactions on energy conversion, Vol. 28, N°3, pp. 682–689. doi:10.1109/TEC.2013.2272244.

Krim Y, Abbes D, Krim S, Mimouni M. F. (2018). Classical vector, first-order sliding mode and high-order sliding-mode control for a grid-connected variable speed wind energy conversion system: A comparative study. Wind Engineering, Vol. 42, N°1, pp. 16– 37. doi:10.1177/0309524X17723202.

Li H, Chen Z. (2008). Overview of different wind generator systems and their comparisons, IET Renewable Power Geneation. Vol. 2, N°2, pp. 123–138. doi: 10.1049/iet-rpg:20070044.

Saihi L, Berbaoui B, Glaoui H. (2020). Robust Control H∞ Fuzzy of a Doubly Fed Induction Generator Integrated to Wind Power System. Majlesi Journal of Electrical Engineering, Vol. 14, N°1.

Serhoud H, Benattous D. (2011). Sensorless Sliding Power Control of Doubly Fed Induction Wind Generator Based on MRAS Observer. International Journal of Electrical and Computer Engineering, Vol. 5, N°8.

Serhoud H, Benattous D. (2012). Sliding mode control of brushless doubly-fed machine used in wind energy conversion system. Revue des Energies Renouvelables, Vol. 15, N°2, pp. 305 – 320. doi: https://doi.org/10.54966/jreen.v15i2.322.

Shanthi P, Uma G, Keerthana M. S. (2017). Effective power transfer scheme for a grid connected hybrid wind/photovoltaic system. IET Renewable Power Generation, Vol. 11, N°7, pp. 1005–1017. doi: 10.1049/iet-rpg.2016.0592.

Tamaarat A, Benakcha A. (2014). Performance of PI controller for control of active and reactive power in DFIG operating in a grid-connected variable speed wind energy conversion system. Frontier in Energy, Vol. 8, N°3, pp. 371–378. doi:10.1007/s11708-014-0318-6.

Tir Z, Abdessemed R. (2014). Control of a wind energy conversion system based on brushless doubly fed induction generator. Revue des Energies Renouvelables, Vol. 17, N°1, pp. 55 – 69.

Zamzoum O, Mourabit Y, Errohha M, Derouich A, El ghzizal A. (2018). Power control of variable speed wind turbine based on doubly fed induction generator using indirect field- oriented control with fuzzy logic controllers for performance optimization, Energy Science and Engineering. Vol. 6, N°5, pp. 408–423. doi: 10.1002/ese3.215.